

# An Autonomous Wall Climbing Robot for Inspection of Reinforced Concrete Structures: SIRCAUR

Gabriela Gallegos Garrido and Tariq Pervez Sattar  
*London South Bank University, London South Bank Innovation Centre  
Granta Park, Great Abington, Cambridge CB21 6AL, UK.*  
[gallegog@lsbu.ac.uk](mailto:gallegog@lsbu.ac.uk), [sattartp@lsbu.ac.uk](mailto:sattartp@lsbu.ac.uk)

\*Corresponding author: [gallegog@lsbu.ac.uk](mailto:gallegog@lsbu.ac.uk)

\*\*Second corresponding author: [sattartp@lsbu.ac.uk](mailto:sattartp@lsbu.ac.uk)

(Received March, 2021 | Accepted June, 2021 | Posted Online July, 2021)

**Abstract:** A wall climbing inspection robot has been designed to climb on safety critical concrete structures by adhering to reinforcement steel bars (rebars) using permanent magnets to generate the adhesion forces. Simulation and experimental validation has been performed to determine the optimum flux focusing magnet configurations with the robot operating on 30 to 35mm of concrete cover over rebars arranged in different patterns. The goal of adhesion force optimization is to be able to carry a ground penetrating radar (GPR) sensor which detects rebar corrosion, concrete delamination and concrete cover deterioration. The autonomous robot uses an ultra-wide band (UWB) localisation system and GPR data to control its motion trajectories to avoid regions where there is insufficient density of rebars. Non-destructive testing (NDT) inspection data acquired by GPR is transmitted wirelessly to a ground station for processing and monitoring by NDT technicians.

**Keywords:** Climbing Robot, GPR NDT, FEA, magnetic adhesion, reinforced concrete, UWB.

## 1. Introduction

Corrosion of structures costs the UK economy approximately 3.5% of its gross domestic product (GDP) annually [1], and results in £100bn yearly for repairs and downtime. Automated methods of corrosion detection and timely repair can reduce the economic impact. Reinforced concrete (R/C) is used throughout the civil engineering industry for roads, bridges, high-rise buildings, dams, cooling towers, etc. Global corrosion repair costs for R/C are about 8% of all corrosion costs [2]. It is estimated that this is about £8bnpa in the UK alone. R/C

inspection is mostly performed manually by constructing expensive scaffolding or by using ropes to reach a test site. The risk of accidents and falls can be reduced by using robotics to perform the inspection. Wall-climbing robot research tries to increase payload capacity, mobility, adhesion forces and to minimise energy consumption [3] [4]. Mobile robots previously designed for concrete inspection are reported in [5] [6] [7].

The robotic development reported here, SIRCAUR, uses a climbing robot to reach test sites on vertical concrete structures to detect rebar corrosion and delamination defects with 100% volume coverage. Tests

have been performed on a concrete wall with rebars at depths of 30-35mm from the surface. The design, prototyping and testing of the robot are illustrated in this paper. The climbing robot was able to climb on concrete structures with rebar density at these depths and the GPR system was able to effectively detect defects.

\*This paper is the extension of a previous published conference article in [12]. The paper has been extended by including the design of our “Flux Focusing Design Toolbox”, built as an application on top of COMSOL Multiphysics to assist the design of permanent magnet adhesion systems for climbing robots. Results of experiments to validate the Toolbox have been included. New experiments have been performed that validate our adhesion system designed for reinforced concrete structures. The following sections describe the crawler’s design. Section 2 describes the design of the adhesion module. Section 3 describes the prototype and the submodules that comprise the crawler’s payload. Finally, Section 4 presents our conclusions.

## 2. Crawler’s design: The adhesion module

To design climbing robots for industrial applications it is important to consider the operating environment and the task to be carried out [3]. Robots that can climb on non-ferrous surfaces tend to employ either suction cups or dynamic vortex adhesion methods which produce a vacuum with fast spinning impellers. These methods require constant energy supply lines for long inspection times which result in long umbilical cables. To climb on structures constructed from ferrous materials, permanent magnets or electromagnets are preferred as they provide higher adhesion forces. Electromagnets control the adhesion force on demand but again require constant energy supply to

maintain adhesion to a structure. Permanent magnet adhesion is the best method for robots climbing on ferrous structures as the force is constant and can be engineered to be high with magnetic flux focusing techniques, does not need the application of power and is fail-safe in the event of power failure to the rest of the robot.

SIRCAUR has been designed to use permanent magnets to adhere to reinforcement bars (rebars) buried in concrete and to use GPR to detect rebar corrosion and other concrete defects. The design of the climbing robot has attempted to increase payload capacity, mobility, adhesion safety and to minimise energy consumption. Permanent magnets are used for the adhesion method for two reasons: (a) The method does not require energy consumption, therefore, avoiding the use of heavy batteries that will increase the payload (b) In case of a power failure, the crawler will remain attached to the surface providing a safety feature.

The next subsections will explain the design of the crawler based on its adhesion module and payload.

### 2.1 The Flux Focusing App

To design a robot that uses permanent magnets to adhere to rebars at distance of 30-40mm from the magnet system, it was necessary to first develop a design tool that predicts the adhesion force when flux focusing techniques are used with different magnet systems comprising of different types of permanent magnets, yokes of different materials and magnet placement configurations.

This section describes the development of the design tool used to select the best magnet system. Analysis of forces on a climbing robot on a vertical plane is given in [4].

Permanent magnet adhesion climbing robots developed for climbing on concrete structures are discussed in [6]. Engineering of these types of climbing robot still remains a difficult trade-off challenge because increasing the payload target requires larger drive motors/gears which in turn increases the weight of the robot which in turn requires more adhesion force to remain attached to a surface. Obtaining sufficient adhesion force to safely carry a target payload when the airgap between magnets and rebars is more than 30mm is the major challenge. A numerical modelling optimization process was carried out to retrofit previously published adhesion mechanisms. To tackle the analysis of this problem COMSOL Multiphysics was used to model the permanent magnet adhesion system.

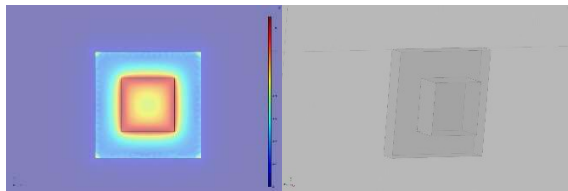


**Figure 1.** Force analysis of N52 Neodymium magnet under ideal conditions.

Adhesion modules were investigated that used several permanent magnets and flux concentrators or “yokes” in different configurations to optimize the adhesion module to give a maximum adhesion force with minimum weight of the module.

## 2.2 Simulation of adhesion force under ideal conditions

To ensure the reliability of modelling, an initial simulation was created to set up a model to compute the adhesion force of the magnets under ideal conditions. This means that the obtained results should match with the manufacturer’s datasheet. Rare-earth neodymium magnets grade N52 and of size 50x50mm with 25mm of thickness are used in the simulation (see Figure 1). From their technical specifications, these magnets have

a holding force of 116kg when in flush contact with a mild steel surface.

This is one of the highest available magnet grades in the market. However, the weight of one magnet at 626 grams is also high.

**Table 1.** Properties used to investigate adhesion modules for COMSOL simulation

Properties	Value
Magnetic induction intensity $B_r$ (T)	1.47
Magnetic coercive force $H_{cb}$ (KA/m)	796
Relative permeability of magnet ( $\mu_r$ )	1.05
Relative permeability of steel plate	1000
Relative permeability of iron yoke	4500

The model comprises one N52 magnet, one steel plate (100x100x15mm) and one iron yoke of the same size as the plate. With the geometry shown in Figure 1 and with material properties listed in Table 1, COMSOL simulations computed the force as 1156.8N (close to specified magnet technical specifications, thus validating the model). It is shown in [8] that adding a yoke of high permeability to close the magnet circuit from one side results in a significant increase in adhesion force on the other side. The results showed that adding an iron yoke of the same size as the steel plate increases the force to 1663.3N. This model was used as a base model to build an App using the COMSOL Application Builder. The App window is shown in Figure 2.

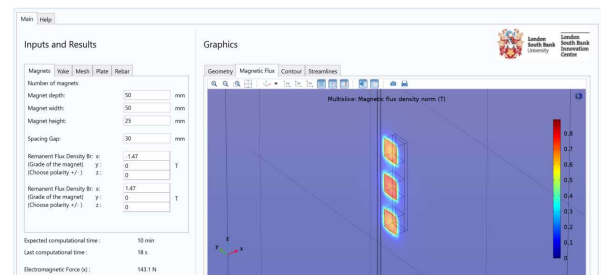


**Figure 2.** FEA Analysis using COMSOL App.

An optimisation process was performed using COMSOL by varying the physical parameters of the magnet-yoke adhesion

module [6]. The parameters varied were the size of the magnet and relative permeability of the ferromagnetic structure. The air gap (distance between ferrous surface and magnet) is another important parameter to design an adhesion system for complex structures [6,7]. The best magnet configuration for maximum adhesion force [5] uses three magnets with N-S-N orientation placed on an iron yoke (Figure 3).

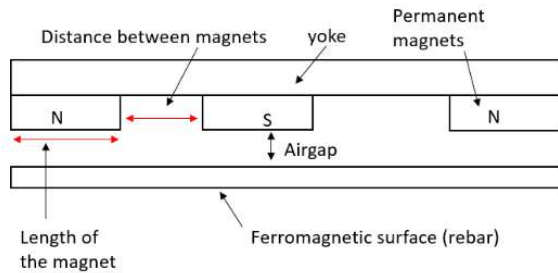


Figure 3. Magnet-Yoke modeling layout.

The simulation model is composed of an iron yoke (250x50x10mm, approximately 960g net weight), three N52 rare earth neodymium magnets are arranged on top of the yoke in a N-S-N configuration with 50mm spacing.

Simulating this magnetic adhesion system (yoke + three magnets) placed over a 12mm steel rebar with 30mm of air gap (concrete cover) predicts an adhesion force of 143.1N.

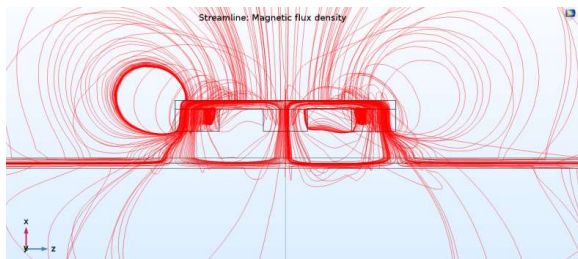


Figure 4. Magnetic flux line behavior of three N52 magnets arranged N-S-N.

The magnetic flux lines are shown in Figure 4. To validate the simulation results, the simulation was validated with an *in-house* experimental test rig. Setup and results are explained next.

### 2.3 Experimental results with in-house test rig

Figure 5 shows the positioning of the magnets on the yoke to construct the adhesion system simulated in section 2.2. The weight of the magnet system was 2.83kg, measured with an industrial scale.

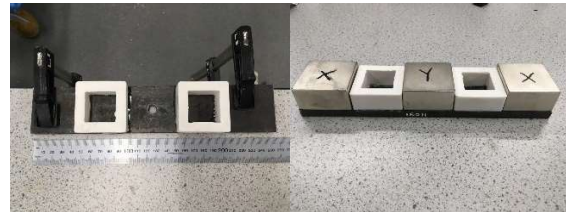


Figure 5. Construction of the magnet system.

An attachment was added to the iron yoke to be able to fix it on the *load cell machine* that performed the force/tension test. The Instron 5567A B723 machine (capable of measuring forces up to 2kN) was calibrated and the test was conducted in accordance with ISO 7500-1:2015. The Instron procedure used was N001.

The magnet system was placed at a distance of 200mm from the rebar on the load cell machine (see Figure 6). The distance was slowly decreased while approaching a 12mm diameter rebar until a 20mm spacing gap was left between the magnets and the rebar. Measured force data was recorded (6 values per second). Measurements were repeated for 16mm and 20mm diameter rebars.

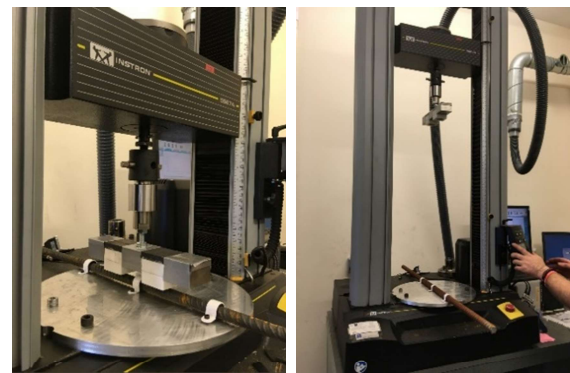
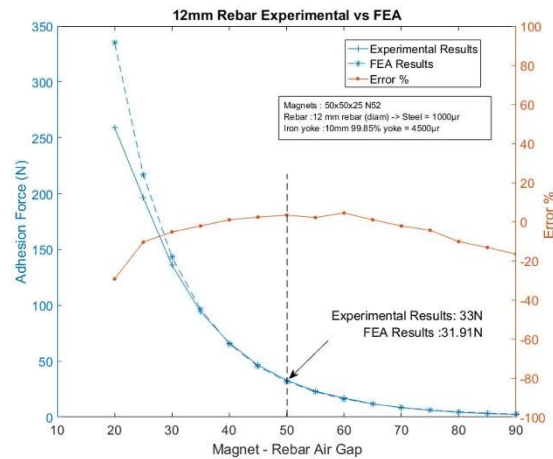


Figure 6. In house test rig using an Instron machine (2kN tension/compression load cell).

For the sake of illustration, in the following sections the results shown were performed on a 12mm diameter rebar.

Most reinforced concrete structures have rebars within a distance of 30-35mm beneath a concrete cover. However, concrete structures exposed to wet conditions have concrete cover that can reach 50mm. Therefore, adhesion force was predicted with simulation and experimental measurement for increasing air gap to the rebar (see Figure 7).

As expected, the adhesion force decreases rapidly with increasing air gap, from around 100N at 35mm to only 31.39N at 50mm. Good agreement between experimental and the COMSOL predictions validates the accuracy of the App.



**Figure 7.** Measured adhesion force and force predicted by FEA with COMSOL.

When the air gap was 30mm, a 5% error was recorded. Minimum error was recorded when the air gap was 40mm (*i.e.* min error of 0.91%). Systematic errors can be the reason for the  $\pm 5\%$  error (*i.e.* when considering the air gap vs forces,  $\pm 1\text{mm}$  can influence the adhesion force significantly). However, these results provide evidence to validate the COMSOL model, and thus give confidence in the application.

## 2.4 Robot R/C potential workspace: Simulations and test rig

In Section 2.2 it is shown that the gap between the magnets and the rebars is the most important determinant of adhesion force. Nevertheless, other parameters such as the diameter, configuration of rebars (*e.g.* a mesh of rebars) and density of ferrous material also influence the adhesion force. British standard BS 850 and Eurocode [9] specify the minimum concrete cover over rebars for different environmental conditions. Most reinforced concrete structures are made of a mesh of rebars as shown in Figure 8.



**Figure 8.** Potential workspace for the climbing robot.

The force estimation application is improved by adding the possibility to choose from a set of rebars (mesh) as the ferrous surface. The gap distance between the rebars and the magnet system (concrete cover) can be changed directly from the application.

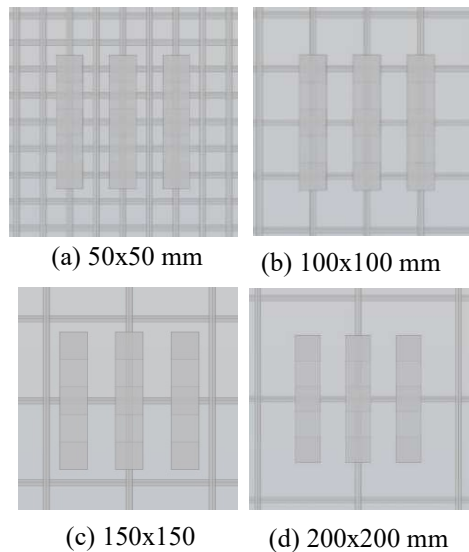


**Figure 9.** Rebar mesh spacing in 4 configurations

For this experiment, four different sizes of mesh were tested (see Figure 9) with three different concrete covers. To cover a large ferrous surface and to achieve the maximum adhesion force, it was decided to develop an arrangement of three yokes in parallel at a distance of 50mm between them. Magnets were arranged in the same way as in Section 2.2. The results are listed in Table 2. As expected, the closer the ferrous surface is to the magnets, the greater is the adhesion force achieved.

**Table 2.** Simulation results with different mesh sizes and concrete covers.

Mesh space	Force at 40mm	Force at 35mm	Force at 30mm
200x200mm	116.7N	159N	225.9N
150x150mm	145N	192.6N	263.3N
100x100mm	252.2N	352.6N	506.3N
50 x 50mm	287.9N	391.4N	546.8N

The aim of this experiment was to determine the type of rebar mesh where the robot will be able to climb as well as its payload capacity. To validate the simulation results, a magnet system consisting of 3 yokes was attached to aluminum brackets as shown in Figure 10. The weight of this system was 10kg.

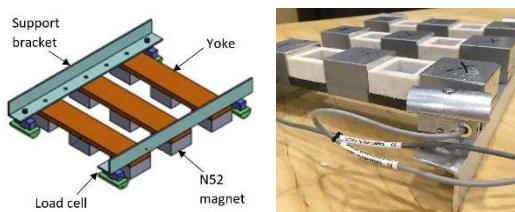


**Figure 10.** Test rig construction with 4 load cells.

To measure adhesion forces, OMEGA mini load cells were attached to each of the four corners. Using an OMEGA summing box and a compatible meter, the total adhesion force applied by the magnet system was measured. A *dynamic* rebar wall was constructed where it was possible to change the spacing between rebars. Three mesh configurations using 12mm diameter rebars were made possible.

The rebar meshes were covered with a fixed plywood board to simulate a concrete cover of 30mm (the relative permeability of dry concrete is practically the same as air and wood). Load cells measurements were recorded with the constructed magnet system placed over the dynamic wall. Comparison of adhesion force measurements performed on the test rig results and predicted forces by FEA from the COMSOL simulation are tabulated in Table 3.

**Table 3.** Estimation of the robot's weight with the proposed magnetic adhesion system

Mesh space with 12mm rebar	FEA magnet force	Load cells force	Max pay-load at 30mm
200x200mm	23.03kg	24.14kg	8.82kg
100x100mm	51.62kg	50.91kg	22.20kg
50x50mm	55.75kg	61.82kg	27.66kg

If coefficient of friction is 0.5 and the total weight of the adhesion system is 10kg, an estimation of the robot's payload capacity is calculated in the last column of Table 3. See analysis in [4].

## 2.5 Real environment testing: Car park

Results from the above experiment give us confidence to apply the adhesion system to a real-world environment. It is a well-known fact that the columns in multi-story car parks are well reinforced.



**Figure 11.** Test on a real reinforce concrete structure: car park column.

Since a reliable method to determine the size of the rebars or their distance was not available, in the first instance the system was

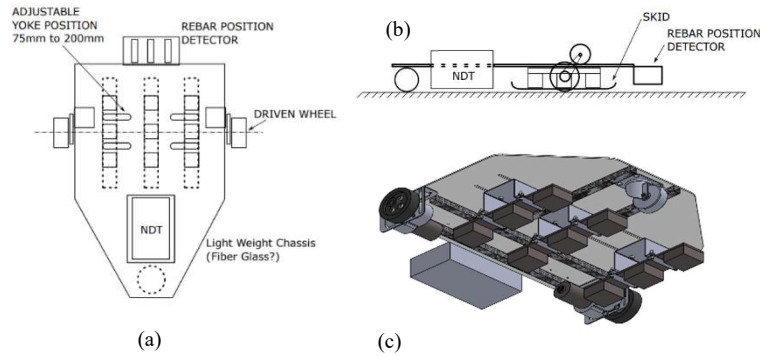


Figure 12: (a),(b) Schematic of the robot, (c) Magnet system

placed on the column to verify that it remained stationary and stuck to the column. Once confirmed that the system was holding, additional weights were incrementally added to the system, as seen in Figure 11, until the system started *sliding*.

While it is not known how much ferrous material was embedded in the car park column, it was established that a robot using this adhesion system will be able to carry a payload of 7.6 kg.

### 3. Crawler's design:

#### The payload

Structure of the physical robot, CAD design, is illustrated in Figure 12. The adhesion module was positioned under the robot to coincide with the rebars. The design was optimized with a series of computer aided design tasks to maintain a balance between the robot's physical parameters such as its weight, payload and the adhesion strength of the magnet module.

#### 3.1 NDT module: GPR

The Ground Penetrating Radar (GPR) is an effective NDT method for concrete structures. This technique has been commercially available since 1970's and numerous studies have been carried out since to develop it for a wide range of concrete inspection applications. It offers a unique technique to characterize surface and subsurface features. Different types of

defects can be identified in rebars and overlaid reinforced concrete decks. It is also used for thickness measurement of concrete members, air void detection, inspection of vertical R/C structures, mapping of reinforcement bar locations and measuring material properties of concrete [10][11]. GPR offers the advantage of high scanning speed and being lightweight (<2kg) and is thus eminently suitable for deployment on a climbing robot. However, its limitations are that it cannot detect delamination, honeycombing, grouting defects or measure variation of the quality of concrete. While other NDT methods can detect these defects they are impractical for deployment on a climbing robot because of weight or because they can only be used in a static position.

Table 4. PicoR-2K GPR specifications

Parameter	Value
Frequency range (at a level of -10 dB)	0.5 - 3.5GHz
Central frequency	1600MHz
Pulse duration	60ps
Pulse amplitude voltage	6V
Pulse repetition frequency	50MHz
Range measurement accuracy	1-2cm

The SIRCAUR project has used the PicoR-2K GPR for the NDT of concrete structures (specification shown in Table 4). The device is designed for subsurface sensing and monitoring of opaque materials. It enables calculation of the thickness of the layers

inside such materials as well as detection and positioning of in-homogeneities within the material.

A laptop running the PicoR 4.3 software was connected via a USB-C cable to the PicoR-2K GPR. A concrete test block was manufactured (Figure 13) with various known degrees of rebar thinning and various sizes of air void, embedded at known depths from the block surface. The concrete test rig block was manufactured and tests were conducted by project partner TWI.

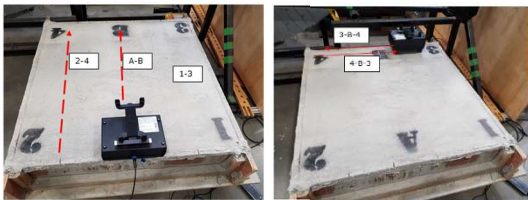


**Figure 13.** (Left) Three scanning paths used to detect air voids. (Right) Scan paths 3-B-4 and 4-B-3 used to detect both air voids and rebars.

Three scanning sequences shown in Figure 13 were used to detect (a) Air voids: GPR moved in directions 1-3, A-B and 2-4. These paths avoided the rebars but passed over the voids created within the concrete block; (b) Rebars: GPR moved in directions 1-A-2 and 3-B-4.

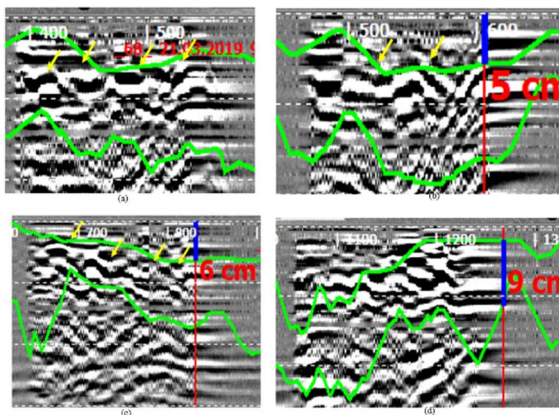


**Figure 14.** (a) Scan path A-B (b) Scan path 2-4 (c) GPR detects four rebars (d) Scan path 4-B-3.

These paths avoided the voids but passed over rebar defects; (c) Rebar and voids: GPR moved in the direction of 3-B-4 and then

from 4-B-3. These trials evaluated the GPR with tightly spaced defects. Results are illustrated in Figure 14.

Explanation of Figure 14: (a) Scan path A-B: Four air voids detected in the scan line. Constant peak heights indicate that the voids are at the same depth; (b) Scan path 2-4 detects two of the three defects in the scan; (c) GPR scan detects four rebars in the concrete block (downward trend of the peaks indicates that the rebars are positioned at increasing depths); (d) Scan path 4-B-3 detects both rebars and air voids. The upwards peak trend indicates that the scan moves from an area where the rebars and voids are at lower position to an area where they are at a higher position.

### 3.2 The prototype

The climbing robot prototype is illustrated in Figure 15. The design was performed by project partners InnoTecUK with the support of TWI and LSBIC. The aim was to keep the whole robot payload including the electronics and the NDT system to less than 20kg. Therefore, the chassis of the robot was made of carbon fiber and aluminum alloy. The robot's control was ROS enabled using a Raspberry Pi.

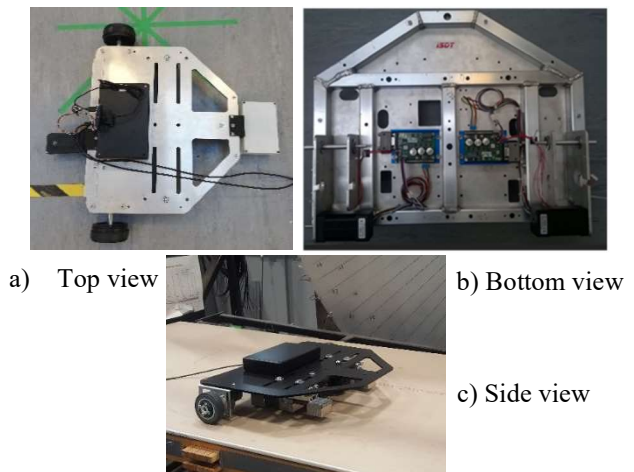


**Figure 15.** Climbing robot different views

A laboratory test climbing surface was created by developing a wall with the same rebar spacing as the simulations. Figure 17 shows the dynamic wall (described in Section 2.3) constructed to perform the trial test. Two climbing tests were conducted with the wall placed horizontally and the climbing robot placed underneath as shown in Figure 16 and the wall erected vertically as shown in Figure 17.



**Figure 16.** (Left) The wall placed horizontally, (Right) Climbing robot on the wall showing that the adhesion force is sufficient to support the payload.

The final configuration used for the trials was with 100x100mm rebar mesh and 12mm diameter rebars. Trial with the crawler upside-down showed that the magnetic adhesion force provided by the permanent magnets was enough to support the weight of the SIRCAUR robot.

### 3.3 The Localization module

A localization system was developed that used the Ultra-Wide Band (UWB) localization technique to provide an accurate measurement of robot position on the wall. The system used the commercially available POZYX™ UWB module which was compatible with the operational microcontroller used for control purposes.

A ROS (Robot Operating System) node was developed to incorporate the localization module into the robot's software architecture. The four beacons of the POZYX system can be seen in Figure 17 at each of the four corners on the wall, which enabled successful location of the robot on the wall.

## 4. Conclusion

SIRCAUR is a lightweight, fast-moving climbing robot system for the inspection of reinforced concrete structures which is easy to deploy and retrieve. The entire structure of robot is built with aluminum alloy and carbon fiber to make it lightweight. Robot structural integrity has been assured with a series of structural analysis experiments using CAD design software (SolidWorks) and FEA software (COMSOL). Adhesion force to carry the robot payload has been optimized by using configurations of Neodymium 52 magnets placed on yokes of high permeability with force predictions made with COMSOL FEA simulations and validated experimentally.



**Figure 17.** Climbing robot tested on vertical wall.

A GPR NDT sensor has been incorporated into the system to detect the presence, location and depth of rebar and air voids in a concrete structure. Laboratory trial tests on a wall engineered to simulate different rebar meshes and rebar depths indicate that the climbing robot can climb on concrete walls when the air gap between the magnet system and rebar is 30 to 35 mm. The adhesion force generated by the permanent magnet system does not require an energy supply and is therefore advantageous for a climbing robot performing NDT on large concrete structures. The GPR system has been shown to detect rebars and air voids and measures both their position and depth.

## Acknowledgments

Innovate UK grant (No: 103668) funded the SIRCAUR project with the following partners: London South Bank University (LSBU/LSBIC), Innovative Technology & Science Ltd (InnotecUK) and TWI Ltd.

Full experimental video is available at - [www.youtube.com/watch?v=nwVGVnlyk4](http://www.youtube.com/watch?v=nwVGVnlyk4)

## References

1. R. A. Market, "Infrastructure Monitoring Market by Technology (Wired and Wireless), Offering (Hardware: Sensors, Data Acquisition Systems; Software & Services), Vertical (Civil infrastructure, Energy), Application & Geography - Global Forecast to 2023," Research and Market, **2018**.
2. Lucintel, "Growth Opportunities in the Global Inspection and Testing Equipment Market in Civil Engineering," **2013**.
3. M. f. Silva and T. J. Machado, "A Survey of Technologies and Applications for Climbing Robots Locomotion and Adhesion," 2010. [Online]. Available: <https://www.intechopen.com/books/climbing-and-walking-robots/a-survey-of-technologies-and-applications-for-climbing-robots-locomotion-and-adhesion>. [Accessed 15 April **2020**].
4. G. Gallegos Garrido, T. Sattar, M. Corsar, R. James and D. Seghier, "Towards safe inspection of long weld lines on ship hulls using an autonomous robot", CLAWAR Conference, **2018**.
5. M. O. F. Howlader and T.P. Sattar, "Finite Element Analysis based Optimization of Magnetic Adhesion Module for Concrete Wall Climbing Robot, "International Journal of Advanced Computer Science and Applications", **vol. 6**, no. 8, pp. 8-18, **2015**.
6. M. O. f. Howlader and T. P. Sattar, "Development of Magnetic Adhesion Based Climbing Robot for Non-Destructive Testing," in *Computer Science and Electronic Engineering Conference (CEEC)*, University of Essex, UK, **2015**.
7. M. O. F. Howlader, "Development of a Wall Climbing Robot and Ground Penetrating Radar System for Non-Destructive Testing of Vertical Safety Critical Concrete Structures," PhD thesis - London South Bank University, London, **2016**.
8. Hussain, S., T. Sattar, and E. Salinas, "Towards Optimum Design of Magnetic Adhesion Wall Climbing Wheeled Robots", 26th International Conference on CAD/CAM, Robotics and Factories of the Future, **2011**.
9. European Standard. Eurocode 2, "Design of Concrete Structures, General Rules".
10. C. P. F. Ulricksen, "Application of impulse radar to civil engineering," Doctoral Thesis, Department of Engineering Geology, Lund University of Technology, Sweden, **1982**.
11. M. Forde, "Ground penetrating radar," Introduction to Nondestructive Evaluation Technologies for Bridges," in Transportation Research Board Pre-conference Workshop, **2004**.
12. G. Gallegos Garrido, M. Dissanayake, T. Sattar, A. Plastropoulos and M. Hashim, "SIRCAUR: Safe Inspection of Reinforced Concrete Structures by Autonomous Robot", CLAWAR Conference, **2020**.